Optimizing Sensitization Processes in Dinuclear Luminescent Lanthanide Oligomers. Selection of Rigid Aromatic Spacers.

Jean-François Lemonnier, Laure Guénée, César Beuchat, Tomasz A. Wesolowski,* Prasun Mukherjee, David H. Waldeck,* Kristy A. Gogick, Stéphane Petoud,* and Claude Piguet*

Supporting Information

(34 pages)

Appendix 1. Determination of the thermodynamic formation constants by ^{1}H NMR.

The ^{1}H NMR spectra of $[Y_2(\mathbf{L}\boldsymbol{k})(hfac)_6]$ (k = 3-5) recorded at the maximum accessible concentrations display signals of the free ligands (Table S1) with those of the twofold dinuclear complexes (Table S16) under slow exchange regime on the NMR time scale (Fig. S10). The thermodynamic equilibria are analyzed according to eq 10.

$$2\ Y(hfac)_3 + \mathbf{L}\boldsymbol{k} \rightleftharpoons [Y_2(\mathbf{L}\boldsymbol{k})(hfac)_6] \qquad \beta_{2,1}^{Y,\mathbf{L}\boldsymbol{k}} \qquad (10)$$

The mass balances are given in eqs S1-S2 while the experimental ratio γ of the integrated ^{1}H NMR signals collected for free ligand (I_L) and for its complex (I_{Y2L}) in the NMR tube can be found in eq S3.

$$\left|L\right|_{tot} = \left|L\right| + \left|Y_2L\right| \qquad (S1)$$

$$\left|Y\right|_{tot} = \left|Y\right| + 2\left|Y_2L\right| \qquad (S2)$$

$$\gamma = \frac{I_{Y_2L}}{I_L} = \frac{\left|Y_2L\right|}{\left|L\right|} \qquad (S3)$$

The introduction of eq S3 into eq S1 yields eq S4, from which the concentrations of the free ligand (eq S5) and of the dinuclear complex (eq S6) can be easily deduced.

$$\left|L\right|_{tot} = \left|L\right|(1+\gamma) \qquad (S4)$$

$$\left|L\right| = \left|L\right|_{tot} / (1+\gamma) \qquad (S5)$$

$$\left|Y_2L\right| = \gamma\left|L\right|_{tot} / (1+\gamma) \qquad (S6)$$

The introduction of eq S6 into eq S2 followed by straightforward algebraic transformations gives

$$\left|Y\right|_{tot} = \left|Y\right| + 2\left[\gamma\left|L\right|_{tot} / (1+\gamma)\right] \Rightarrow \left|Y\right| = \frac{\left|Y\right|_{tot}(1+\gamma) - 2\gamma\left|L\right|_{tot}}{(1+\gamma)} \qquad (S7)$$

The final introduction of Eqs S5-S7 into the expression of the thermodynamic formation constant leads to

$$\beta_{2,1}^{Y,L} = \frac{\left|Y_2L\right|}{\left|L\right|\left|Y\right|^2} = \frac{\gamma(1+\gamma)^2}{\left[\left|Y\right|_{tot}(1+\gamma) - 2\gamma\left|L\right|_{tot}\right]^2} \qquad (S8)$$

The uncertainties affecting $\beta_{2,1}^{Y,L}$ are estimated by using standard error propagation schemes[49] applied to eq S8 and using the uncertainties affecting $\left|L\right|_{tot}$, $\left|Y\right|_{tot}$ and γ.

Appendix 2. Correction of the absorption spectrum of [Gd_2(L*k*)(hfac)$_6$] for partial dissociation in solution.

$$2\ \mathrm{Ln(hfac)_3} + \mathbf{L}\boldsymbol{k} \rightleftharpoons [\mathrm{Ln_2}(\mathbf{L}\boldsymbol{k})(\mathrm{hfac})_6] \qquad \beta_{2,1}^{\mathrm{Ln},\mathbf{L}\boldsymbol{k}} \qquad (10)$$

Once the formation constant $\beta_{2,1}^{\mathrm{Ln},\mathbf{L}\boldsymbol{k}}$ is at hand (eq 10), the speciation in solution is easily obtained from the mass balances given in eqs S9 and S10 (C_{Lk} and C_{Ln} are the total concentrations of ligand, respectively of metallic unit Ln(hfac)$_3$) and the law of mass action (eq S11).

$$C_{\mathrm{Lk}} = |\mathrm{L}k| + |\mathrm{Ln_2L}k| \Rightarrow |\mathrm{Ln_2L}k| = C_{\mathrm{Lk}} - |\mathrm{L}k| \qquad (S9)$$

$$C_{\mathrm{Ln}} = |\mathrm{Ln}| + 2|\mathrm{Ln_2L}k| \Rightarrow |\mathrm{Ln}| = C_{\mathrm{Ln}} - 2|\mathrm{Ln_2L}k| = C_{\mathrm{Ln}} - 2\left(C_{\mathrm{Lk}} - |\mathrm{L}k|\right) \qquad (S10)$$

$$\beta_{2,1}^{\mathrm{Ln},\mathrm{L}k} = \frac{|\mathrm{Ln_2L}k|}{|\mathrm{L}k||\mathrm{Ln}|^2} \qquad (S11)$$

Introduction of eqs S9 and S10 into eq S11 yields

$$\beta_{2,1}^{\mathrm{Ln},\mathrm{L}k} = \frac{C_{\mathrm{Lk}} - |\mathrm{L}k|}{|\mathrm{L}k|\left[C_{\mathrm{Ln}} - 2\left(C_{\mathrm{Lk}} - |\mathrm{L}k|\right)\right]^2} \qquad (S12)$$

Straightforward, but tedious algebraic transformations eventually leads to

$$4\beta_{2,1}^{\mathrm{Ln,L}}|\mathrm{L}k|^3 + 4\beta_{2,1}^{\mathrm{Ln,L}}|\mathrm{L}k|^2\left(C_{\mathrm{Ln}} - 2C_{\mathrm{Lk}}\right) + \beta_{2,1}^{\mathrm{Ln,L}}|\mathrm{L}k|\left[\left(C_{\mathrm{Ln}} - 2C_{\mathrm{Lk}}\right)^2 + 1\right] - C_{\mathrm{Lk}} = 0 \qquad (S13)$$

For any mixture of ligand and metal, the solution of the cubic eq S13 provides the concentration of the free ligand, from which those of the free metal and free complex can be deduced with eqs S9 and S10. The total absorbance A_{tot} at a wavelength λ is given by the Lambert-Beer relationship (eq S14), where $\varepsilon_{\mathrm{Ln}}^{\lambda}$, $\varepsilon_{\mathrm{L}k}^{\lambda}$ and $\varepsilon_{\mathrm{Ln2Lk}}^{\lambda}$ are the molar extinction coefficients of Ln(hfac)$_3$, **L*k*** and [Ln_2(**L*k***)(hfac)$_6$], respectively, and l is the pathlength of the analytic cell. According that the absorption spectra of Ln(hfac)$_3$ (Fig. S11) and **L*k*** (Fig S3) can be recorded independently, the absorption of the pure complex corrected for dissociation is obtained by using eq S15 and the experimental absorbance A_{tot} recorded for any $C_{\mathrm{Ln}}/C_{\mathrm{Lk}}$ mixture (Fig. 7).

$$A_{\mathrm{tot}} = l\sum_n \varepsilon_n^{\lambda}|n| \qquad (S14)$$

$$\varepsilon_{\mathrm{Ln2Lk}}^{\lambda} = \frac{\left(A_{\mathrm{tot}}/l\right) - \varepsilon_{\mathrm{Ln}}^{\lambda}|\mathrm{Ln}| - \varepsilon_{\mathrm{L}k}^{\lambda}|\mathrm{L}k|}{|\mathrm{Ln_2L}k|} \qquad (S15)$$

Appendix 3. Synthesis of the complexes [Ln(hfac)$_3$diglyme] (Ln = Eu, Gd, Y).

For midrange lanthanides (Ln = Eu, Gd), the corresponding lanthanide oxide Ln_2O_3 (2.55 mmol), diglyme (0.75 ml, 5.2 mmol) and Hhfac (0.75 ml, 14 mmol) were refluxed in toluene (20 ml) for 10 h. The resulting turbid solution was filtered and evaporated to dryness. The yellow wax was sublimed under vacuum (2.10^{-4} bar) at 140°C to give 3.2 g of [Ln(hfac)$_3$diglyme] as colourless crystals (yield 60-70%).

[Eu(hfac)$_3$diglyme] NMR ^{1}H (400 MHz $CDCl_3$) : -0.5 (br, 3H), 2.47 (s, 4H), 11.65 (br, 4H), 26.48 (br, 6H). Elemental analyses: calcd for $Eu(C_5F_6O_2H)_3(C_6H_{14}O_3)$ %C 27.80, %H 1.89. Found %C 27.79, %H 1.90.

[Gd(hfac)$_3$diglyme] Elemental analyses: calcd for $Gd(C_5F_6O_2H)_3(C_6H_{14}O_3)$ %C 27.80, %H 1.89. Found %C 27.58, %H 1.87.

For small lanthanides (Ln = Y), $YCl_3{\cdot}6H_2O$ (3.7 g, 12.2 mmol) were dissolved in water (150 mL). Aq. NaOH (14 mL, 4M, 56 mmol) were added. The resulting gel was filtered, washed with water and dried under vacuum to give 3.9 g of white solid. Suspension in hexane (420 mL) containing Hhfac (2.8 mL, 57 mmol) and diglyme (1.95 mL, 13.9 mmol) yielded a pink solution which was refluxed for 2 h, then evaporated to dryness. The resulting waxy pink solid was sublimed under vacuum at 110°C to give 7.58 g of colourless crystals (8.97 mmol yield 82%). ^{1}H NMR (400 MHz $CDCl_3$): 6.09 (s, 3H), 3.91 (t, ^3J=5.0Hz, 4H), 3.80 (t, ^3J=5.0Hz, 4H), 3.47 (s, 6H). Elemental analyses: calcd for $Y(C_5F_6O_2H)_3(C_6H_{14}O_3)$ %C 29.88, %H 2.03. Found %C 29.82, %H 2.07.

Appendix 4. Synthesis of compound 1.

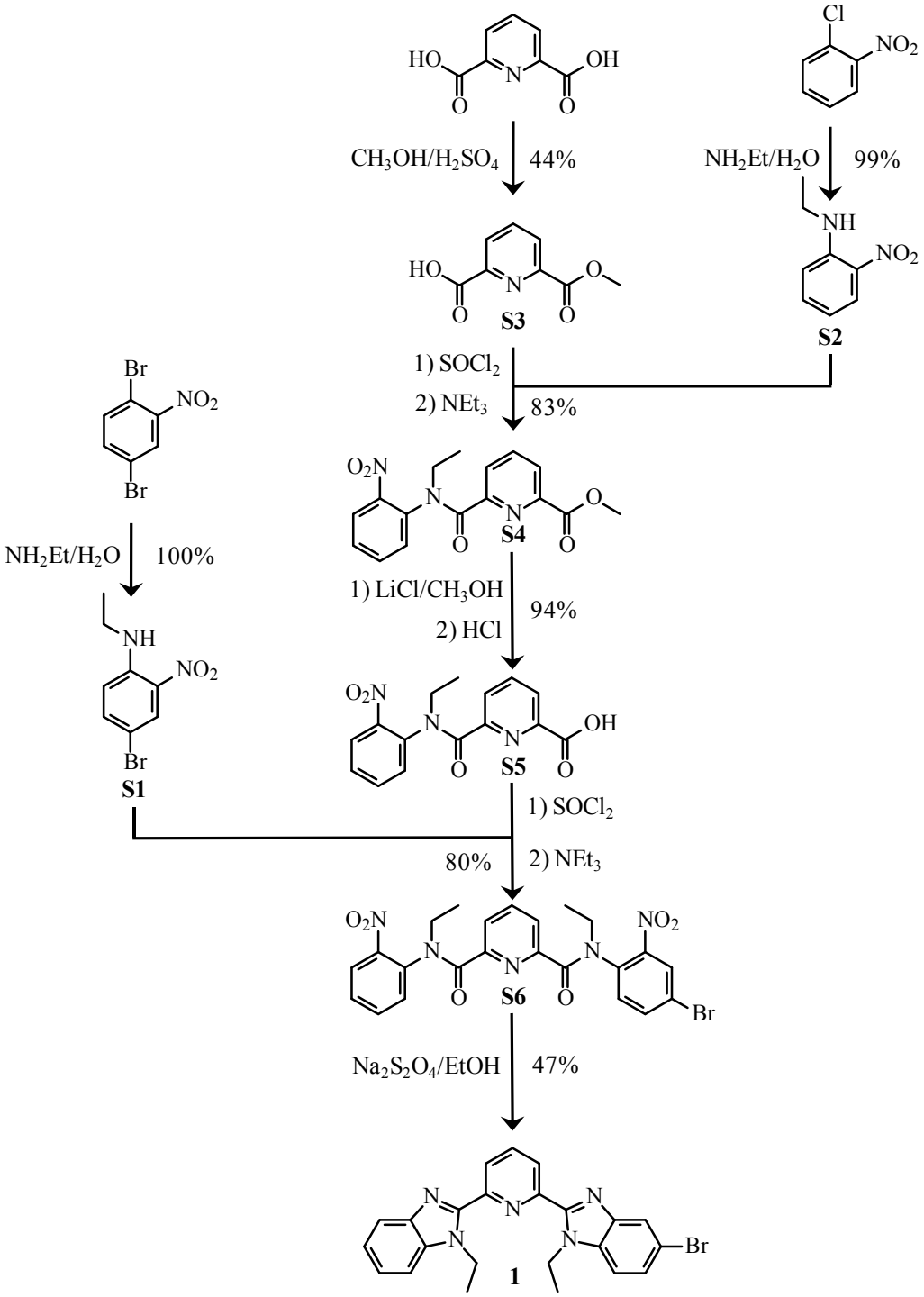

Scheme S1 Synthesis of compound **1**.

Preparation of S1. 1,4-dibromo-2-nitrobenzene (5 g, 17.8 mmol) and aq. ethylamine (60 mL, 70%) were heated at 100°C for 24 h. in a sealed vessel. The resulting red solution was concentrated by evaporation and partitioned between dichloromethane (250 mL) and half-sat. aq. NH_4Cl (250 250mL). The aq. phase was separated, extracted with dichloromethane (2x100 mL). The combined

organic phases were dried (Na_2SO_4), filtered and evaporated to dryness to give S1 as red crystals (4.3 g, 17.8 mmol, yield = 100%). ^{1}H NMR ($CDCl_3$; 400 MHz): δ = 1.36 (t, ^3J = 7.1 Hz, 3H), 3.35 (q, ^3J=7.1 Hz, 2H), 6.76 (d, ^3J = 9.2 Hz, 1H), 7.49 (dd, ^3J = 9.2 Hz, ^4J = 2.3 Hz, 1H), 7.99 (s, 1H),.8.31 (d, ^4J = 2.3 Hz, 1H)**.**

Preparation of S2. 1-chloro-2-nitrobenzene (10.0 g, 63 mmol) and aq. ethylamine (60 mL, 70%) were heated at 105°C for 24 h. in a sealed vessel. The resulting orange solution was concentrated by evaporation and partitioned between dichloromethane (150 mL) and half-sat. aq. NH_4Cl (150mL). The aq. phase was separated, extracted with dichloromethane (2x100 mL). The combined organic phases were dried (Na_2SO_4), filtered and evaporated to dryness to give **S2** (10.4 g, 62 mmol, yield = 99%) as a yellow oil. ^{1}H NMR ($CDCl_3$; 400 MHz): δ = 8.17 (d, ^3J = 8 Hz, 1H), 7,97 (s, 1H), 7.43 (t, ^3J = 8 Hz, 1H), 6.85 (d, ^3J = 8 Hz, 1H), 6.63 (t, ^3J = 8 Hz, 1H), 3.37 (q, ^3J = 7 Hz, 1H), 1.38 (t, ^3J = 7Hz).

Preparation of S3. 2,6 dipicolinic acid (10.26 g, 60 mmol) and conc. sulfuric acid (1 mL) were refluxed in methanol/water (50mL:50 mL) for 25 min.. The resulting mixture was poured into sat. aq. $NaHCO_3$ (500 mL) and the aqueous phase was washed with dichloromethane (3x100 mL). The pH was then adjusted to pH = 4 with aq. HCl and the aq. phase was extracted with dichloromethane (4x200 mL). The combined organic phases were dried (Na_2SO_4), filtered and evaporated to dryness to give **S3** (4.8 g, 26.5 mmol, yield = 44%) as a white powder. ^{1}H NMR (d_6-DMSO; 400 MHz): δ = 4.41 (s, 3H), 8.71 (t, ^3J = 8Hz, 1H), 8.79 (dd, ^3J = 8Hz, ^4J = 1 Hz, 1H), 8.81 (dd, ^3J = 8Hz, ^4J = 1 Hz, 1H), 12.30 (s, 1H).

Preparation of S4. Thionyl chloride (35 mL, 57 g, 487 mmol), **S3** (3.4 g, 18.6 mmol) and *N*,*N*-dimethylformamide (500 µl) were refluxed under an inert atmosphere for 30 min. Evaporation to dryness followed by drying under vacuum provided a grey solid, which was dissolved in dry dichloromethane (50 mL). Dichloromethane (40 mL) containing **S2** (3.32 g, 20 mmol) and triethyl amine (6 mL) was slowly added and the mixture refluxed for 12h. After evaporation to dryness, the residue was partitioned between dichloromethane (300 mL) and half-sat. aq. NH_4Cl (300 mL). The

aq. phase was separated, extracted with dichloromethane (2x100 mL) and the combined organic phases were dried (Na_2SO_4), filtered and evaporated to dryness. The residual oil was purifed by column chromatography (Silicagel, CH_2Cl_2/MeOH 100:0→99:1) to yield **S4** (5.1 g, 15.5 mmol, yield = 83%) as a yellow oil. ^{1}H NMR (400 MHz, $CDCl_3$) δ 8.18 (d, ^3J = 7.8 Hz, 1H), 8.10 (d, ^3J = 7.8 Hz, 1H), 7.98 (t, ^3J = 7.8 Hz, 1H), 7.87 (d, ^3J = 8.1 Hz, 1H), 7.63 (t, ^3J = 7.7 Hz, 1H), 7.48 (t, ^3J = 7.7 Hz, 1H), 7.39 (d, ^3J = 7.9 Hz, 1H), 4.19 (m, 1H), 3.83 (m, 1H), 1.28 (t, ^3J = 7.2 Hz, 3H). ESI-MS: *m/z* 330.3 ($[M+H]^+$).

Preparation of S5. A solution of $LiOH·H_2O$ (3.27 g, 77.8 mmol) in methanol/water (100mL:50mL) was added dropwise to a cooled (0°C) solution of **S4** (5.1 g, 15.5 mmol) in methanol (50 mL). The mixture was stirred for 3h at 0°C, then poured into water (300 mL). The aq. phase was washed with dichloromethane (3x100 mL) and the pH set to pH = 2 with conc. hydrochloric acid. The resulting aq. phase was extracted with dichloromethane (4x100 mL). The combined organic phases were dried (Na_2SO_4), filtered and evaporated to dryness to yield **S5** (4.39 g, 13.9 mmol, yield = 90%) as a white powder. ^{1}H NMR ($CDCl_3$; 400 MHz): δ = 1.25 (t, ^3J = 7.1Hz, 3H), 3.77 (q, ^3J = 7.1Hz, 1H), 4.15 (q, ^3J = 7.1Hz, 1H), 6.76 (d, ^3J = 9.2 Hz, 1H), 7.49 (dd, ^3J = 9.2 Hz, ^4J = 2.3 Hz, 1H), 7.97 (t, ^3J = 8Hz, 1H), 7.99 (s, 1H) 8.10 (d, ^3J = 8.2Hz, 1H), 8.14 (d, ^3J = 8.2Hz, 1H), 8.31 (d, ^3J = 8.2Hz, 1H), 9.81 (s, 1H).

Preparation of S6. Thionyl chloride (50 mL, 81.5 g, 695 mmol), **S5** (9.4 g, 30 mmol) and N,N-dimethylformamide (500 μl) were refluxed under an inert atmosphere for 30 min. Evaporation to dryness followed by drying under vacuum provided a grey solid, which was dissolved in dry dichloromethane (150 mL). Dichloromethane (60 mL) containing **S1** (8.8 g, 36 mmol) and triethylamine (7 mL) was slowly added, and the mixture was refluxed for 24 h. After evaporation to dryness, the brown residue was partitioned between dichloromethane (300 mL) and half-sat. aq. NH_4Cl (300 mL). The aq. layer was separated, extracted with dichloromethane (3x150 mL) and the combined organic phases were dried (Na_2SO_4), filtered and evaporated to dryness. The residual

solid was purifed by column chromatography (Silicagel, CH_2Cl_2/MeOH 100:0→98:2) to yield **S6** (13.0 g, 24 mmol, yield = 80%) as a yellow solid. ESI-MS: m/z 542.3 ($[M+H]^+$).

Preparation of 1. Sodium dithionite (41 g, 200 mmol), **S6** (13.0 g, 24 mmol) in ethanol:DMF (50 mL:50mL) were heated at 80°C for 5 minutes then water (60 ml) is added. The mixture was further refluxed under an inert atmosphere for 24 h. The resulting yellow turbid solution was evaporated. The resulting yellow foam was partitioned between dichloromethane (300 mL) and half-sat. aq. $NaHCO_3$ (300 mL). The organic phase was dried (Na_2SO_4), filtered and evaporated to dryness. The residual solid was purified by column chromatography (Silicagel, CH_2Cl_2/MeOH 100:0→98:2) to yield **1** (5.0 g, 11.2 mmol, yield = 47%) as a pale grey solid. ^{1}H NMR (400 MHz, $CDCl_3$) δ 8.36 (dd, ^3J = 7.9, ^4J=1.1 Hz, 1H), 8.33 (dd, ^3J=7.9Hz, ^4J=1.1 Hz, 1H), 8.06 (t, ^3J = 7.9 Hz, 1H), 8.01 (d, ^3J = 1.8 Hz, 1H), 7.88 (dd,^3J=6.1Hz, ^4J=2.0Hz, 1H), 7.49 (dd, ^3J=6.1Hz, ^4J=2.0Hz, 1H), 7.47 (dd, ^3J=8.7Hz, ^4J=1.8Hz, 1H), 7.36 (m, 3H), 4.80 (q, ^3J=7.4Hz, 2H), 4.78 (q, ^3J=7.4Hz, 2H), 1.37 (t, . ^3J=7.4Hz, 3H), 1.36 (t, . ^3J=7.4Hz, 3H). ESI-MS (positive mode/CH_3OH): *m/z* 447.5 ($[M+H]^+$)

Table S1. ^{1}H NMR Shifts (in ppm with Respect to TMS) for the Ligands **L3**-**L5** in $CDCl_3$ at 293 K [a]

Protons	**L3**	**L4**	**L5**
H1	7.78	7.64	7.69
H2	7.38	7.38	7.38
H3	7.38	7.38	7.38
H4	7.56	7.51	7.50
H5	4.84	4.82	4.82
H6	1.37	1.39	1.39
H7	8.34	8.39	8.36
H8	8.12	8.09	8.08
H9	8.37	8.39	8.38
H10	4.87	4.85	4.85
H11	1.39	1.42	1.42
H12	7.65	7.64	7.56
H13	7.72	7.89	7.89
H14	8.08	8.12	8.14
H15	7.82	7.40	7.15

[a] Numbering is shown in Scheme 2.

Table S2 Elemental Analyses for $[Ln_2(\mathbf{L}\boldsymbol{k})(hfac)_6]$ Complexes (Ln = Eu, Gd, Y).

Compound	MM/ $gmol^{-1}$	%C found	%H found	%N found	%C calc	%H calc	%N calc
$[Eu_2(\mathbf{L3})(hfac)_6]$	2355.2	41.19	2.26	5.95	41.82	2.14	5.94
$[Gd_2(\mathbf{L3})(hfac)_6]$	2365.8	41.87	2.17	5.85	41.63	2.13	5.92
$[Y_2(\mathbf{L3})(hfac)_6]$	2229.1	44.49	2.48	6.06	44.18	2.26	6.28
$[Eu_2(\mathbf{L4})(hfac)_6]$	2391.2	40.92	2.02	5.80	41.19	2.09	5.86
$[Gd_2(\mathbf{L4})(hfac)_6]$	2408.1	41.39	2.08	5.42	41.00	2.01	5.83
$[Y_2(\mathbf{L4})(hfac)_6]$	2265.1	44.49	2.48	6.06	43.48	2.14	6.18
$[Eu_2(\mathbf{L5})(hfac)_6]$	2415.3	41.74	2.27	5.74	41.77	2.25	5.80
$[Gd_2(\mathbf{L5})(hfac)_6]$	2425.8	41.52	2.29	5.72	41.59	2.24	5.77
$[Y_2(\mathbf{L5})(hfac)_6]$	2265.1	41.87	2.17	5.85	44.07	2.38	6.12

Table S3 Summary of Crystal Data, Intensity Measurements and Structure Refinements for $[Yb_2(\mathbf{L3})(hfac)_6]$ (**1**), $[Y_2(\mathbf{L3})(hfac)_6]$ (**2**), $[Yb_2(\mathbf{L4})(hfac)_6]$ (**3**), $[Eu_2(\mathbf{L5})(hfac)_6]$ (**4**).

	$[Yb_2(\mathbf{L3})(hfac)_6]$	$[Y_2(\mathbf{L3})(hfac)_6]$	$[Yb_2(\mathbf{L4})(hfac)_6]$	$[Eu_2(\mathbf{L5})(hfac)_6]$
Empirical formula	$C_{82}H_{50}F_{36}N_{10}O_{12}Yb_2$	$C_{82}H_{50}F_{36}N_{10}O_{12}Y_2$	$C_{82}H_{48}F_{38}N_{10}O_{12}Yb_2$	$C_{84}H_{54}Eu_2F_{36}N_{10}O_{14}$
Formula weight	2397.40	2229.14	2433.38	2415.29
Temperature	200(2)K	180(2)K	200(2)K	150(2)K
Wavelength	0.71073 Å	0.71073 Å	0.71069 Å	0.71073 Å
Crystal System, Space group	Monoclinic, *C* 2/*c*	Monoclinic, *C* 2/*c*	Triclinic, *P* -1	Triclinic, *P*-1
Unit cell dimensions	*a* = 31.108(5) Å	*a* = 31.076(3) Å	*a* = 12.5860(8) Å	*a* = 12.1392(7) Å
	b = 15.439(3) Å	*b* = 15.3146(9) Å	*b* = 12.6093(8) Å	*b* = 12.7080(7) Å
	c = 23.333(3) Å	*c* = 23.392(2) Å	*c* = 14.5497(10) Å	*c* = 16.7807(10) Å
	α = 90°	α = 90°	α = 103.816(5)°	α = 75.761(5)°
	β = 106.151(11)°.	β = 106.094(7)°.	β = 93.852(5)°.	β = 70.952(5)°.
	γ = 90°	γ = 90°	γ = 103.810(5)°	γ = 65.580(4)°
Volume in Å^3	10764(3)	10696.5(15)	2158.5(2)	2209.4(2)
Z, Calculated density	4, 1.479 Mg/m^3	4, 1.384 Mg/m^3	1, 1.872 Mg/m^3	1, 1.815 Mg/m^3
Absorption coefficient	1.844 mm^{-1}	1.197 mm^{-1}	2.303 mm^{-1}	1.553 mm^{-1}
F(000)	4688	4440	1188	1190
Theta range for data collection	1.48 to 27.00 °	1.49 to 28.03 °	1.68 to 28.02 °	1.91 to 29.21 °
Limiting indices	-39<=*h*<=23,	-40<=*h*<=40,	-15<=*h*<=16,	-16<=*h*<=16,
	-19<=*k*<=19,	-18<=*k*<=20,	-16<=*k*<=16,	-17<=*k*<=16,
	-29<=*l*<=29	-29<=*l*<=30	-19<=*l*<=19	-22<=*l*<=22

Reflections collected / unique	22056 / 10330	38008 / 12820	23736 / 10270	28515 / 11041
	[R(int) = 0.0797]	[R(int) = 0.0774]	[R(int) = 0.0315]	[R(int) = 0.0641]
Completeness to theta	27.00°/ 87.8 %	28.03°/ 99.0%	28.02°/ 98.2 %	29.21°/ 91.9 %
Data / restraints / parameters	10330 / 1 / 520	12820 / 24 / 584	10270 / 13 / 672	11041 / 0 / 661
Goodness-of-fit on F^2	1.148	1.312	1.318	0.986
Final R indices [$I>2\sigma(I)$]	R_1 = 0.0875,	R_1 = 0.0923,	$R1$ = 0.0309,	R_1 = 0.0381,
	ωR_2 = 0.2112	ωR_2 = 0.2106	$\omega R2$ = 0.0857	ωR_2 = 0.0784
R indices (all data)	R_1 = 0.1504,	R_1 = 0.1461,	$R1$ = 0.0332,	R_1 = 0.0495,
	ωR_2 = 0.2387	ωR_2 = 0.2267	$\omega R2$ = 0.0866	ωR_2 = 0.0830
Largest diff. peak and hole	1.054 and -2.307 e.Å^{-3}	0.886 and -0.577 e.Å^{-3}	1.447 and -1.237 e.Å^{-3}	0.734 and -1.538 e.Å^{-3}

Table S4 Selected Bond Distances (Å), Bond Angles (°) in [Yb_2(**L3**)$(hfac)_6$] (**1**).

Bond distances (Å)

Atom 1	Atom 2	Distance	Atom 1	Atom 2	Distance
Yb(1)	O(1)	2.304(8)	Yb(1)	N(1)	2.440(10)
Yb(1)	O(2)	2.319(8)	Yb(1)	N(4)	2.446(10)
Yb(1)	O(6)	2.336(9)	Yb(1)	O(5)	2.509(10)
Yb(1)	O(4)	2.367(7)	Yb(1)	N(3)	2.519(10)
Yb(1)	O(3)	2.418(11)	Yb(1)	Yb(1)’	12.624(2)

Symmetry operation (’) -*x*+1,*y*,-*z*+1/2.

Angles (°)

At. 1	At. 2	At. 3	angle	At. 1	At. 2	At. 3	angle
O(1)	Yb(1)	O(2)	79.4(3)	O(4)	Yb(1)	N(4)	69.0(4)
O(1)	Yb(1)	O(6)	79.8(3)	O(3)	Yb(1)	N(4)	133.6(3)
O(2)	Yb(1)	O(6)	134.8(3)	N(1)	Yb(1)	N(4)	130.7(3)
O(1)	Yb(1)	O(4)	138.1(4)	O(1)	Yb(1)	O(5)	70.0(3)
O(2)	Yb(1)	O(4)	78.5(3)	O(2)	Yb(1)	O(5)	67.1(3)
O(6)	Yb(1)	O(4)	138.9(3)	O(6)	Yb(1)	O(5)	68.1(3)
O(1)	Yb(1)	O(3)	69.7(4)	O(4)	Yb(1)	O(5)	130.2(3)
O(2)	Yb(1)	O(3)	68.2(3)	O(3)	Yb(1)	O(5)	123.7(3)
O(6)	Yb(1)	O(3)	137.5(3)	N(1)	Yb(1)	O(5)	135.2(3)
O(4)	Yb(1)	O(3)	69.2(3)	N(4)	Yb(1)	O(5)	72.7(3)
O(1)	Yb(1)	N(1)	80.0(3)	O(1)	Yb(1)	N(3)	136.3(3)
O(2)	Yb(1)	N(1)	139.1(4)	O(2)	Yb(1)	N(3)	144.2(3)
O(6)	Yb(1)	N(1)	74.5(4)	O(6)	Yb(1)	N(3)	67.6(3)
O(4)	Yb(1)	N(1)	94.3(3)	O(4)	Yb(1)	N(3)	71.9(3)
O(3)	Yb(1)	N(1)	71.6(3)	O(3)	Yb(1)	N(3)	117.1(4)
O(1)	Yb(1)	N(4)	142.7(4)	N(1)	Yb(1)	N(3)	64.2(4)
O(2)	Yb(1)	N(4)	84.5(3)	N(4)	Yb(1)	N(3)	66.5(3)
O(6)	Yb(1)	N(4)	88.3(4)	O(5)	Yb(1)	N(3)	119.3(4)

Table S5 Selected Least-Squares Planes Data for in $[Yb_2(\mathbf{L3})(hfac)_6]$ (**1**).

Least-Squares Planes

Least-squares planes description	Abbreviation	Max. deviation/Å	Atom
Benzimidazole 2	Bz2		
C1 C2 C3 C4 C5 C6 N2 C7 N1		0.038(1)	N2
Pyridine	Py		
N3 C10 C11 C12 C13 C14		0.022(1)	C13
Benzimidazole 4	Bz4		
C15 N5 C16 C17 C18 C19 C20 C21 N4		0.041(1)	C17
Phenyl	Ph		
C24 C25 C26 C24’ C25’ C26’		0.000	

Interplanar angles (°)

	Bz2	Py	Bz4	Ph
Bz2		6.17(3)	20.78(2)	43.13(4)
Py			21.69(3)	41.03(6)
Bz4				25.26(4)
Ph				

Table S6 Selected Bond Distances (Å), Bond Angles (°) in $[Y_2(\mathbf{L3})(hfac)_6]$ (**2**).

Bond distances (Å)

Atom 1	Atom 2	Distance	Atom 1	Atom 2	Distance
Y(1)	O(2)	2.325(4)	Y(1)	O(5)	2.487(4)
Y(1)	O(1)	2.340(4)	Y(1)	N(1)	2.487(5)
Y(1)	O(6)	2.353(4)	Y(1)	N(4)	2.493(5)
Y(1)	O(4)	2.377(4)	Y(1)	N(3)	2.568(4)
Y(1)	O(3)	2.448(4)	Y(1)	Y(1)’	12.573(3)

Symmetry operation (’) -*x*+1,*y*,-*z*+3/2.

Angles (°)

At. 1	At. 2	At. 3	angle	At. 1	At. 2	At. 3	angle
O(2)	Y(1)	O(1)	78.58(16)	O(4)	Y(1)	N(1)	93.56(14)
O(2)	Y(1)	O(6)	79.85(16)	O(3)	Y(1)	N(1)	70.97(15)
O(1)	Y(1)	O(6)	136.04(14)	O(5)	Y(1)	N(1)	136.49(15)
O(2)	Y(1)	O(4)	138.15(16)	O(2)	Y(1)	N(4)	142.40(14)
O(1)	Y(1)	O(4)	78.03(14)	O(1)	Y(1)	N(4)	86.20(14)
O(6)	Y(1)	O(4)	138.91(14)	O(6)	Y(1)	N(4)	88.15(16)
O(2)	Y(1)	O(3)	71.22(16)	O(4)	Y(1)	N(4)	69.18(14)
O(1)	Y(1)	O(3)	68.50(14)	O(3)	Y(1)	N(4)	133.74(15)
O(6)	Y(1)	O(3)	136.88(16)	O(5)	Y(1)	N(4)	72.96(14)
O(4)	Y(1)	O(3)	68.07(14)	N(1)	Y(1)	N(4)	128.70(14)
O(2)	Y(1)	O(5)	69.45(14)	O(2)	Y(1)	N(3)	137.16(16)
O(1)	Y(1)	O(5)	67.34(13)	O(1)	Y(1)	N(3)	144.25(15)
O(6)	Y(1)	O(5)	69.33(14)	O(6)	Y(1)	N(3)	67.36(14)
O(4)	Y(1)	O(5)	129.60(13)	O(4)	Y(1)	N(3)	72.02(14)
O(3)	Y(1)	O(5)	125.05(13)	O(3)	Y(1)	N(3)	115.62(13)
O(2)	Y(1)	N(1)	81.98(15)	O(5)	Y(1)	N(3)	119.32(13)
O(6)	Y1	N(1)	73.96(15)	O(1)	Y1	N(1)	138.82(15)

Table S7 Selected Least-Squares Planes Data for in $[Y_2(\mathbf{L3})(hfac)_6]$ (**4**).

Least-Squares Planes

Least-squares planes description	Abbreviation	Max. deviation /Å	Atom
Benzimidazole 2	Bz2		
C1 C2 C3 C4 C5 C6 N2 C7 N1		0.018(1)	C7
Pyridine	Py		
N3 C10 C11 C12 C13 C14		0.018(1)	C13
Benzimidazole 4	Bz4		
C15 N5 C16 C17 C18 C19 C20 C21 N4		0.015(1)	C19
Phenyl	Ph		
C24 C25 C26 C24’ C25’ C26’		0.000	

Interplanar angles (°)

	Bz2	Py	Bz4	Ph
Bz2		6.96(3)	21.80(2)	44.32(4)
Py			23.55(3)	42.95(6)
Bz4				25.00(4)
Ph				

Table S8 Selected Bond Distances (Å), Bond Angles (°) in [Yb_2(**L4**)$(hfac)_6$] (**3**).

Bond distances (Å)

Atom 1	Atom 2	Distance	Atom 1	Atom 2	Distance
Yb(1)	O(5)	2.297(2)	Yb(1)	O(3)	2.469(2)
Yb(1)	O(2)	2.308(2)	Yb(1)	N(4)	2.473(3)
Yb(1)	O(1)	2.314(2)	Yb(1)	N(1)	2.479(3)
Yb(1)	O(4)	2.333(2)	Yb(1)	N(3)	2.526(3)
Yb(1)	O(6)	2.438(2)	Yb(1)	Yb(1)’	14.77(1)

Symmetry operation (’) -x,-y+1,-z+1.

Angles (°)

At. 1	At. 2	At. 3	angle	At. 1	At. 2	At. 3	angle
O(5)	Yb(1)	O(2)	137.33(9)	O(4)	Yb(1)	N(4)	71.09(9)
O(5)	Yb(1)	O(1)	77.93(9)	O(6)	Yb(1)	N(4)	70.71(9)
O(2)	Yb(1)	O(1)	76.40(9)	O(3)	Yb(1)	N(4)	135.03(9)
O(5)	Yb(1)	O(4)	143.48(9)	O(5)	Yb(1)	N(1)	69.09(9)
O(2)	Yb(1)	O(4)	76.64(9)	O(2)	Yb(1)	N(1)	141.02(8)
O(1)	Yb(1)	O(4)	133.28(9)	O(1)	Yb(1)	N(1)	86.04(9)
O(5)	Yb(1)	O(6)	70.09(9)	O(4)	Yb(1)	N(1)	91.70(9)
O(2)	Yb(1)	O(6)	69.40(9)	O(6)	Yb(1)	N(1)	136.11(9)
O(1)	Yb(1)	O(6)	70.28(8)	O(3)	Yb(1)	N(1)	70.56(9)
O(4)	Yb(1)	O(6)	131.50(9)	N(4)	Yb(1)	N(1)	129.75(9)
O(5)	Yb(1)	O(3)	127.34(9)	O(5)	Yb(1)	N(3)	72.63(9)
O(2)	Yb(1)	O(3)	70.57(8)	O(2)	Yb(1)	N(3)	139.49(8)
O(1)	Yb(1)	O(3)	66.87(9)	O(1)	Yb(1)	N(3)	144.10(9)
O(4)	Yb(1)	O(3)	68.45(8)	O(4)	Yb(1)	N(3)	71.07(8)
O(6)	Yb(1)	O(3)	126.45(9)	O(6)	Yb(1)	N(3)	116.50(8)
O(5)	Yb(1)	N(4)	97.04(9)	O(3)	Yb(1)	N(3)	117.05(8)
O(2)	Yb(1)	N(4)	81.85(8)	N(4)	Yb(1)	N(3)	65.12(9)
O(1)	Yb(1)	N(4)	139.95(9)	N(1)	Yb(1)	N(3)	64.65(9)

Table S9 Selected Least-Squares Planes Data for in $[Yb_2(\mathbf{L4})(hfac)_6]$ (**3**).

Least-Squares Planes

Least-squares planes description	Abbreviation	Max. deviation /Å	Atom
Benzimidazole 2	Bz2		
C1 C2 C3 C4 C5 C6 N2 C7 N1		0.033(1)	C7
Pyridine	Py		
N3 C10 C11 C12 C13 C14		0.013(1)	C13
Benzimidazole 4	Bz4		
C15 N5 C16 C17 C18 C19 C20 C21 N4		0.031(1)	N4
Phenyl	Ph		
C24 C25 C26 C24’ C25’ C26’		0.000	

Interplanar angles (°)

	Bz2	Py	Bz4	Ph
Bz2		11.80(3)	21.33(2)	65.4(1)
Py			18.90(3)	70.9(1)
Bz4				54.1(1)
Ph				

Table S10 Selected Bond Distances (Å), Bond Angles (°) in $[Eu_2(\mathbf{L5})(hfac)_6]$ (**4**).

Bond distances (Å)

Atom 1	Atom 2	Distance	Atom 1	Atom 2	Distance
Eu(1)	O(3)	2.404(2)	Eu(1)	O(5)	2.453(2)
Eu(1)	O(6)	2.407(2)	Eu(1)	N(4)	2.580(2)
Eu(1)	O(2)	2.428(2)	Eu(1)	N(1)	2.581(3)
Eu(1)	O(7)	2.431(2)	Eu(1)	N(3)	2.610(3)
Eu(1)	O(4)	2.440(2)	Eu(1)	Eu(1)'	14.928(3)

Symmetry operation (') -x,-y,-z+1.

Angles (°)

At. 1	At. 2	At. 3	angle	At. 1	At. 2	At. 3	angle
O(3)	Eu(1)	O(6)	134.69(8)	O(7)	Eu(1)	N(4)	143.54(8)
O(3)	Eu(1)	O(2)	70.43(8)	O(4)	Eu(1)	N(4)	81.50(8)
O(6)	Eu(1)	O(2)	139.36(8)	O(5)	Eu(1)	N(4)	77.49(8)
O(3)	Eu(1)	O(7)	142.65(8)	O(3)	Eu(1)	N(1)	87.15(8)
O(6)	Eu(1)	O(7)	72.03(8)	O(6)	Eu(1)	N(1)	75.79(8)
O(2)	Eu(1)	O(7)	73.52(8)	O(2)	Eu(1)	N(1)	74.55(8)
O(3)	Eu(1)	O(4)	135.10(8)	O(7)	Eu(1)	N(1)	74.07(9)
O(6)	Eu(1)	O(4)	76.00(8)	O(4)	Eu(1)	N(1)	137.24(8)
O(2)	Eu(1)	O(4)	109.22(8)	O(5)	Eu(1)	N(1)	142.15(8)
O(7)	Eu(1)	O(4)	67.02(8)	N(4)	Eu(1)	N(1)	125.74(8)
O(3)	Eu(1)	O(5)	70.42(8)	O(3)	Eu(1)	N(3)	65.68(8)
O(6)	Eu(1)	O(5)	141.22(8)	O(6)	Eu(1)	N(3)	69.23(8)
O(2)	Eu(1)	O(5)	69.40(8)	O(2)	Eu(1)	N(3)	118.21(8)
O(7)	Eu(1)	O(5)	105.55(8)	O(7)	Eu(1)	N(3)	126.84(8)
O(4)	Eu(1)	O(5)	68.15(8)	O(4)	Eu(1)	N(3)	132.56(8)
O(3)	Eu(1)	N(4)	73.32(8)	O(5)	Eu(1)	N(3)	127.45(8)
O(6)	Eu(1)	N(4)	83.21(8)	N(4)	Eu(1)	N(3)	63.56(8)
O(2)	Eu(1)	N(4)	137.12(8)	N(1)	Eu(1)	N(3)	62.25(8)

Table S11 Selected Least-Squares Planes Data for in $[Eu_2(\mathbf{L5})(hfac)_6]$ (**4**).

Least-Squares Planes

Least-squares planes description	Abbreviation	Max. deviation /Å	Atom
Benzimidazole 2	Bz2		
C1 C2 C3 C4 C5 C6 N2 C7 N1		0.018(1)	C4
Pyridine	Py		
N3 C10 C11 C12 C13 C14		0.010(1)	C14
Benzimidazole 4	Bz4		
C15 N5 C16 C17 C18 C19 C20 C21 N4		0.015(1)	C16
Phenyl	Ph		
C24 C25 C26 C24’ C25’ C26’		0.000	

Interplanar angles (°)

	Bz2	Py	Bz4	Ph
Bz2		15.16(3)	35.57(2)	68.25(5)
Py			23.06(3)	63.71(4)
Bz4				45.34(4)
Ph				

Table S12 Bond Distances ($\delta_{i,j}$) Bond Valences ($\nu_{\mathrm{Ln},j}$)[a] and Total Atom Valence (V_{Ln})[b] in the Crystal Structure of [Yb_2(**L3**)(hfac)$_6$] (**1**).

Atom [c]	Donor type	$\delta_{\mathrm{Ln},j}$ / Å	$\nu_{\mathrm{Ln},j}$	
O1	hfac	2.304	0.388	
O2	hfac	2.319	0.373	
O3	hfac	2.418	0.285	
O4	hfac	2.367	0.328	
O5	hfac	2.509	0.223	Average O-hfac
O6	hfac	2.336	0.356	0.33(6)
N1	bzim	2.44	0.362	
N3	py	2.519	0.292	Average N-heterocyclic
N4	bzim	2.446	0.356	0.34(4)
		V_{Ln}	2.964	

[a] $\nu_{\mathrm{Ln},j} = e^{\left[\left(R_{\mathrm{Ln}j} - \delta_{\mathrm{Ln},j}\right)/b\right]}$, whereby $\delta_{\mathrm{Ln},j}$ is the Ln-donor atom j distance. The valence bond parameters $R_{\mathrm{Ln,N}}$ and $R_{\mathrm{Ln,O}}$ are taken from refs 41e,f and b = 0.37Å. [b] $V_{\mathrm{M}} = \sum_j \nu_{\mathrm{M},j}$.[41] [c] Numbering taken from Figure 7a.

Table S13 Bond Distances ($\delta_{i,j}$) Bond Valences ($\nu_{\mathrm{Ln},j}$)[a] and Total Atom Valence (V_{Ln})[b] in the Crystal Structure of [Yb_2(**L4**)(hfac)$_6$] (**3**).

Atom [c]	Donor type	$\delta_{\mathrm{Ln},j}$ / Å	$\nu_{\mathrm{Ln},j}$	
O1	hfac	2.314	0.378	
O2	hfac	2.308	0.384	
O3	hfac	2.469	0.249	
O4	hfac	2.333	0.359	
O5	hfac	2.297	0.396	Average O-hfac
O6	hfac	2.438	0.270	0.34(6)
N1	bzim	2.479	0.326	
N3	py	2.526	0.287	Average N-heterocyclic
N4	bzim	2.473	0.331	0.32(2)
		V_{Ln}	2.980	

[a] $\nu_{\mathrm{Ln},j} = e^{\left[\left(R_{\mathrm{Ln}j} - \delta_{\mathrm{Ln},j}\right)/b\right]}$, whereby $\delta_{\mathrm{Ln},j}$ is the Ln-donor atom j distance. The valence bond parameters $R_{\mathrm{Ln,N}}$ and $R_{\mathrm{Ln,O}}$ are taken from refs 41e,f and b = 0.37Å. [b] $V_{\mathrm{M}} = \sum_j \nu_{\mathrm{M},j}$.[41] [c] Numbering taken from Figure 7b.

Table S14 Bond Distances ($\delta_{i,j}$) Bond Valences ($\nu_{\mathrm{Ln},j}$)[a] and Total Atom Valence (V_{Ln})[b] in the Crystal Structure of [Eu_2(**L5**)(hfac)$_6$] (**4**).

Atom [c]	Donor type	$\delta_{\mathrm{Ln},j}$ / Å	$\nu_{\mathrm{Ln},j}$	
O1	hfac	2.428	0.349	
O2	hfac	2.404	0.372	
O3	hfac	2.44	0.337	
O4	hfac	2.453	0.326	
O5	hfac	2.407	0.369	Average O-hfac
O6	hfac	2.431	0.346	0.35(2)
N1	bzim	2.58	0.322	
N3	py	2.61	0.297	Average N-heterocyclic
N4	bzim	2.581	0.321	0.31(1)
		V_{Ln}	3.039	

[a] $\nu_{\mathrm{Ln},j} = e^{\left[\left(R_{\mathrm{Ln},j} - \delta_{\mathrm{Ln},j}\right)/b\right]}$, whereby $\delta_{\mathrm{Ln},j}$ is the Ln-donor atom j distance. The valence bond parameters $R_{\mathrm{Ln,N}}$ and $R_{\mathrm{Ln,O}}$ are taken from ref refs 41e,f and b = 0.37Å. [b] $V_{\mathrm{M}} = \sum_j \nu_{\mathrm{M},j}$.[41] [c] Numbering taken from Figure 7c.

Table S15. Ligand Speciation for the Complexes [Y_2(**L*k***)(hfac)$_6$] (k = 1-4) in Solution as Inferred from the Stability Constants Determined by ^{1}H NMR (293 K).

Ligand	Solvent	$\log\left(\beta_{2,1}^{\mathrm{Y,L}k}\right)$	$\left\|\mathbf{L}k\right\|_{\mathrm{tot}}$ /mM	**%L*k*** complex
L3	CD_3CN	7.3(4)	1.6 [a]	84
L3	CD_3CN	7.3(4)	0.1	29
L3	CD_3CN	7.3(4)	0.01	0.8
L4	CD_3CN	6.6(3)	1.6 [a]	74
L4	CD_3CN	6.6(3)	0.1	11
L4	CD_3CN	6.6(3)	0.01	0.2
L5	CD_3CN	8.4(5)	0.6 [a]	87
L5	CD_3CN	8.4(6)	0.1	29
L5	CD_3CN	8.4(6)	0.01	8

[a] Maximum solubility.

Table S16 ^{1}H NMR Shifts (in ppm with Respect to TMS) for the Complexes $[Y_2(\mathbf{L}k)(hfac)_6]$ (k = 3-5) in CD_3CN at 293 K [a]

Protons	$[Y_2(\mathbf{L3})(hfac)_6]$	$[Y_2(\mathbf{L4})(hfac)_6]$	$[Y_2(\mathbf{L5})(hfac)_6]$
H1	8.03	8.02	7.97
H2	7.31	7.30	7.30
H3	7.46	7.46	7.46
H4	7.82	7.73	7.69
H5	4.74	4.73	4.73
H6	1.66	1.66	1.66
H7	8.35	8.35	8.34
H8	8.49	8.49	8.49
H9	8.32	8.33	8.31
H10	4.79	4.79	4.79
H11	1.71	1.71	1.72
H12	7.70	7.70	7.64
H13	7.88	7.84	7.76
H14	8.25	8.10	8.03
H15	7.77	7.30	6.95
H(hfac)	5.91	5.89	5.88

[a] Numbering is shown in Scheme S2 and Figure S10.

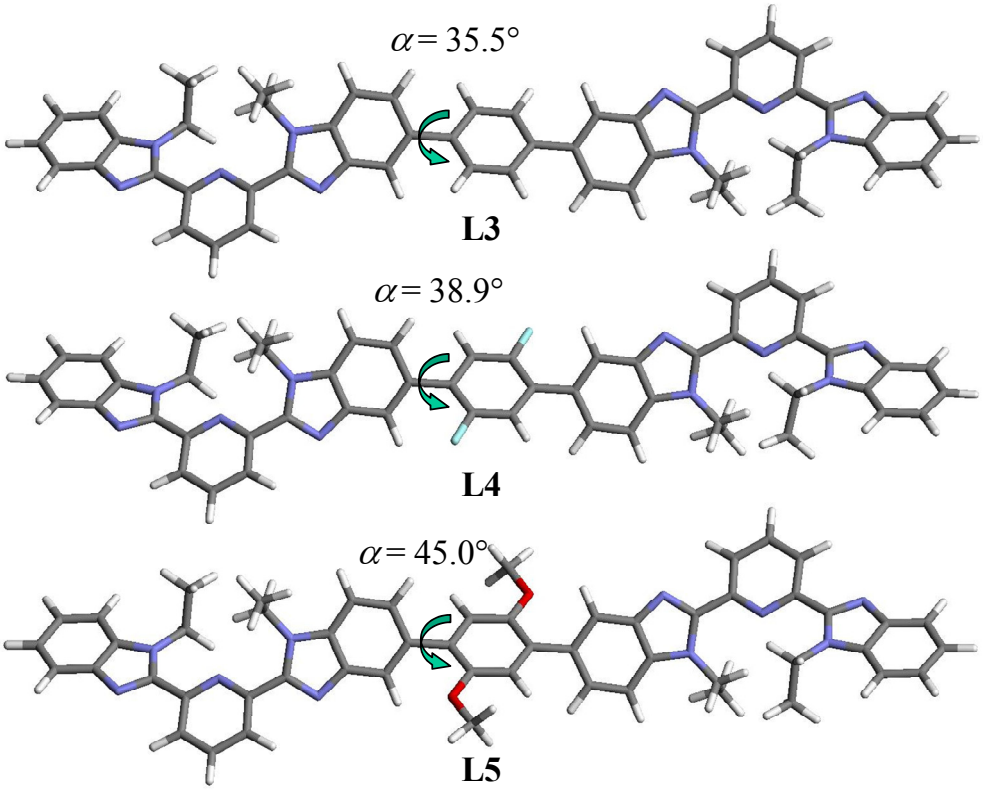

Figure S1 Gas-phase TD-DFT optimized structures for the centro-symmetrical ligands **L3**-**L5** (α = phenyl-benzimidazole interplanar angle).

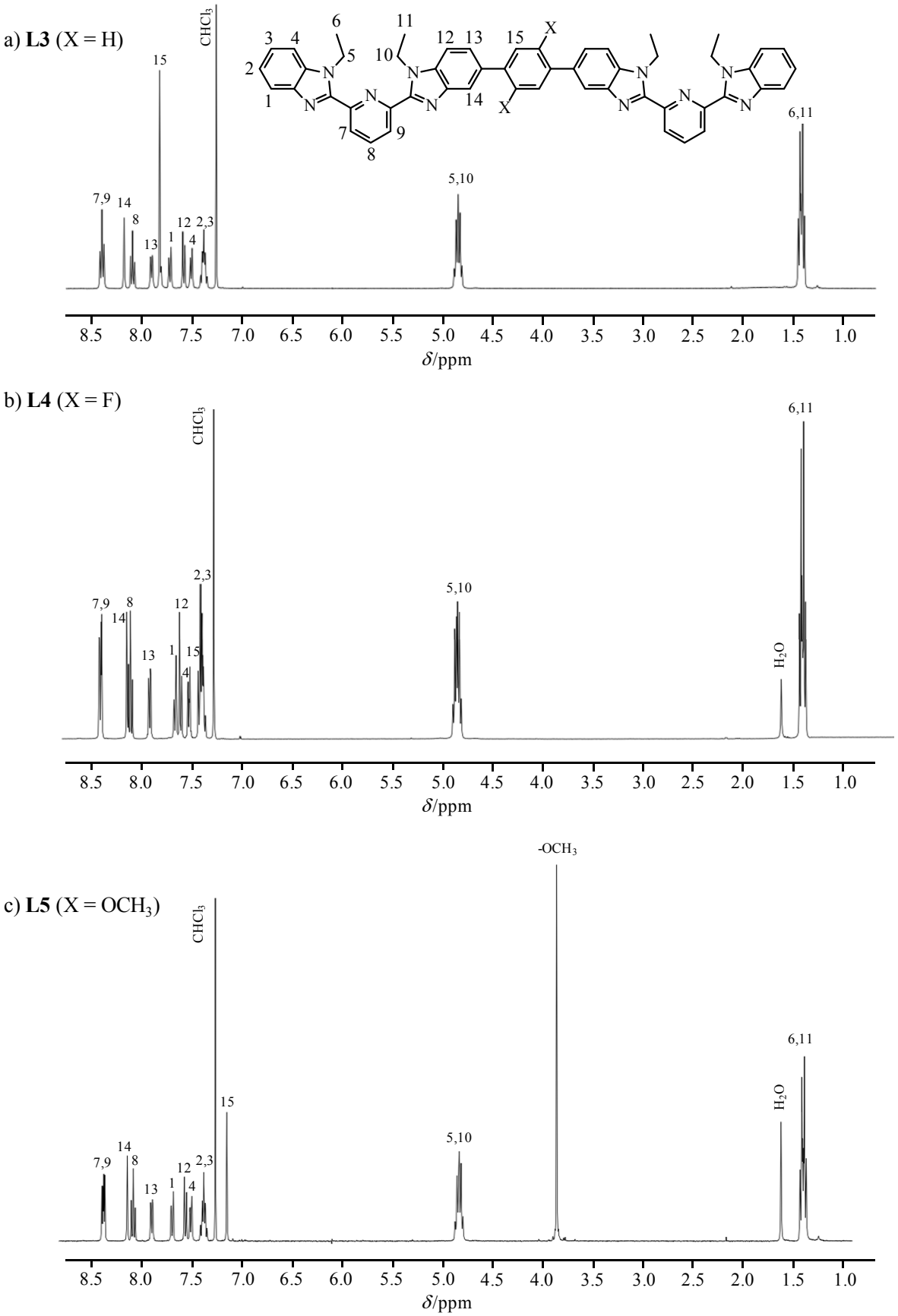

Figure S2 ^{1}H NMR spectra of the ligands **L3**-**L5** ($CDCl_3$, 293 K).

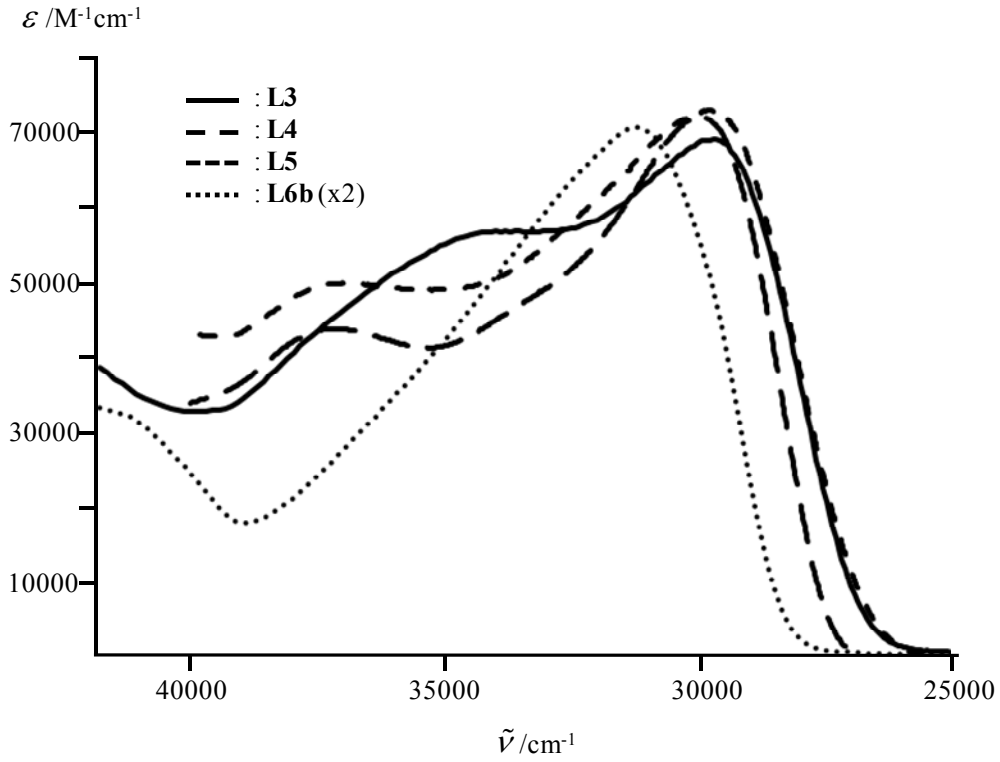

Figure S3 Electronic absorption spectra of ligands **L3**-**L6** (10^{-4} M, CH_2Cl_2, 293 K). For **L6b**, the molar absorption coefficients have been doubled for comparison purpose.

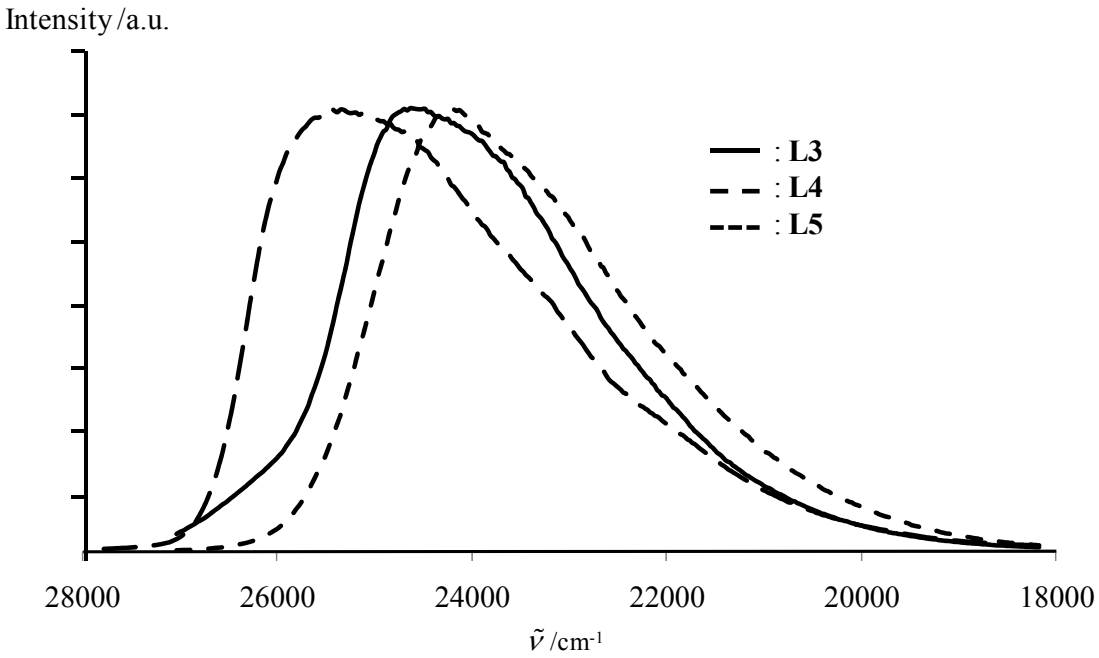

Figure S4 Fluorescence emission spectra of **L3**-**L5** in frozen solution (10^{-4} M in CH_2Cl_2, 77 K).

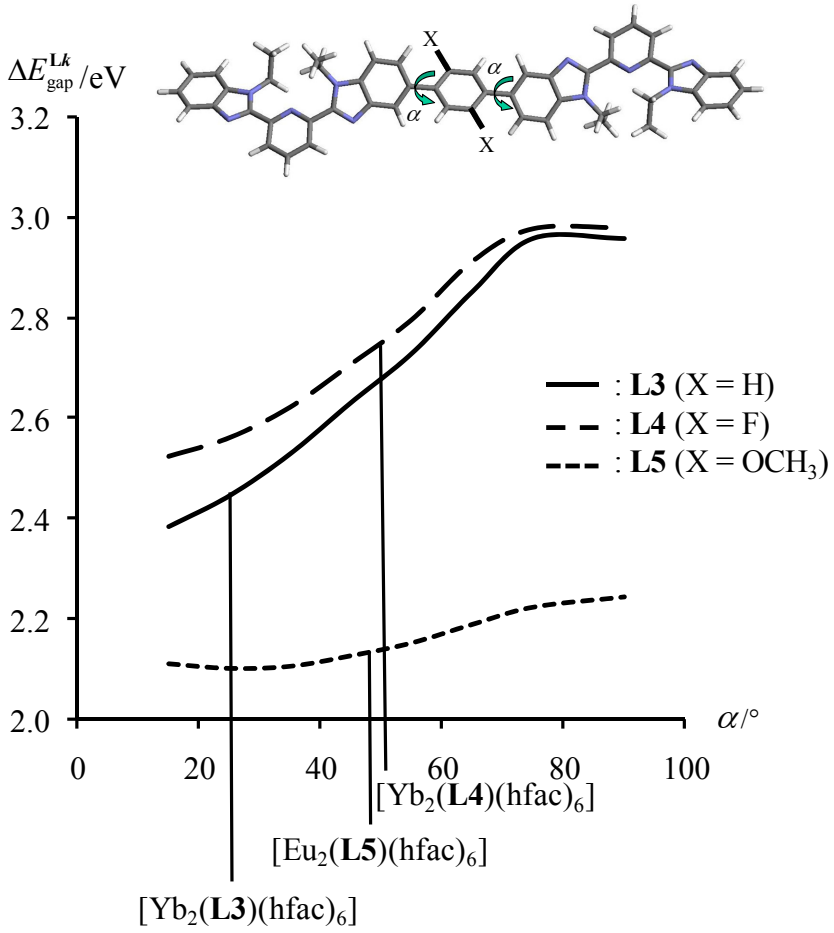

Figure S5 Gas-phase DFT computed HOMO-LUMO gap ΔE_{gap}^{Lk} for the ligands **L3**-**L5** as a function of the interplanar phenyl-benzimidazole angle α. The geometries found for the spacers in the crystal structures of [Ln(**L*k***)(hfac)$_6$] are shown with vertical full lines.

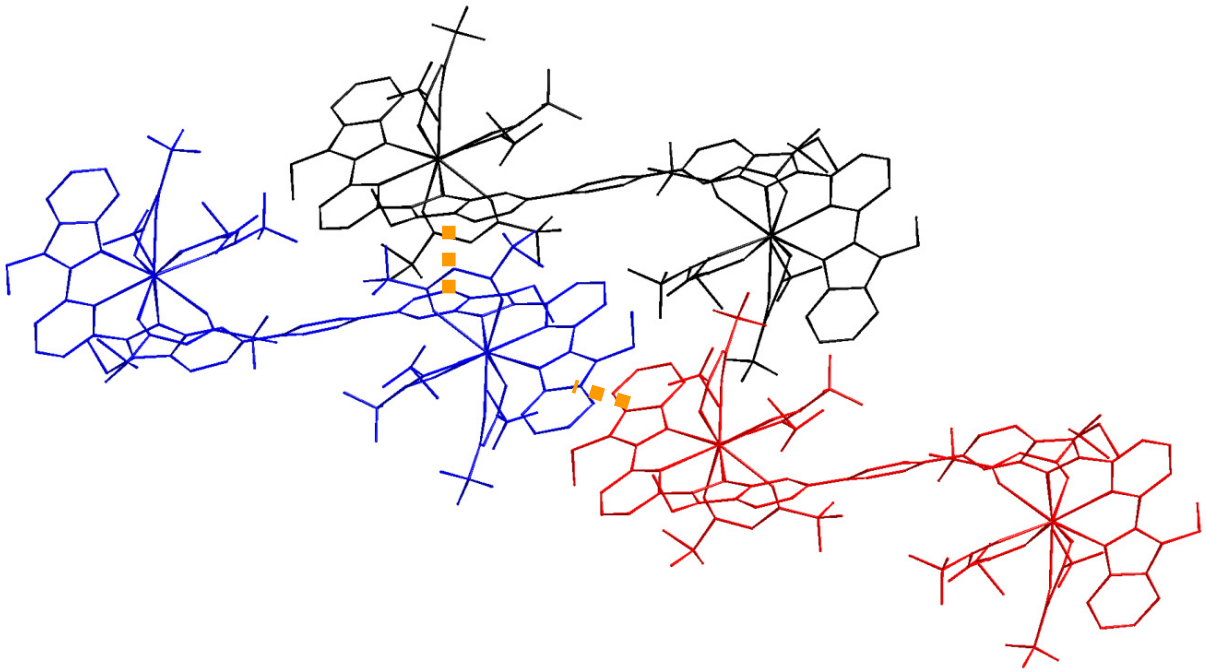

Figure S6 Intermolecular π-stacking interactions found in $[Yb_2(\mathbf{L3})(hfac)_6]$ (**1**) Each complex is involved in four intermolecular benzimidazole···benzimidazole interactions (d = 3.42 Å) with neighbouring molecules related by inversion centres.

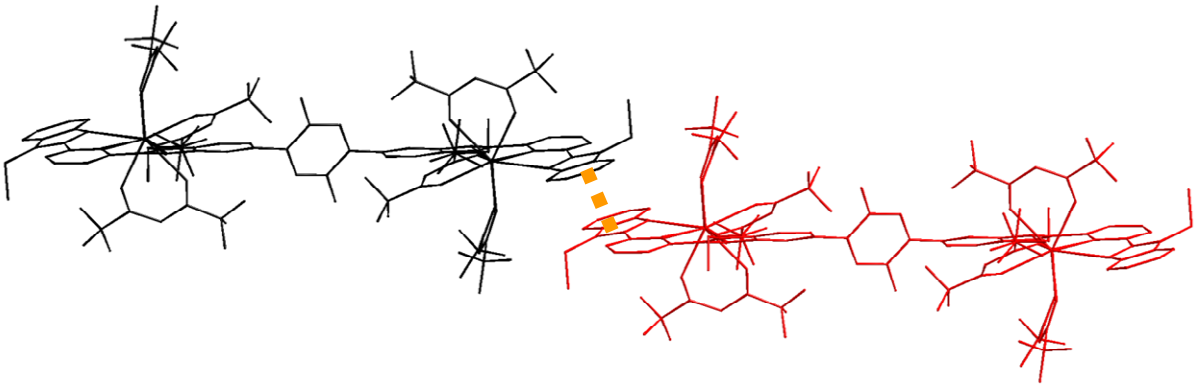

Figure S7 Intermolecular π-stacking interactions found in $[Yb_2(\mathbf{L4})(hfac)_6]$ (**3**) Each complex is involved in two intermolecular benzimidazole···benzimidazole interactions (d = 3.33 Å) with neighbouring molecules related by inversion centres.

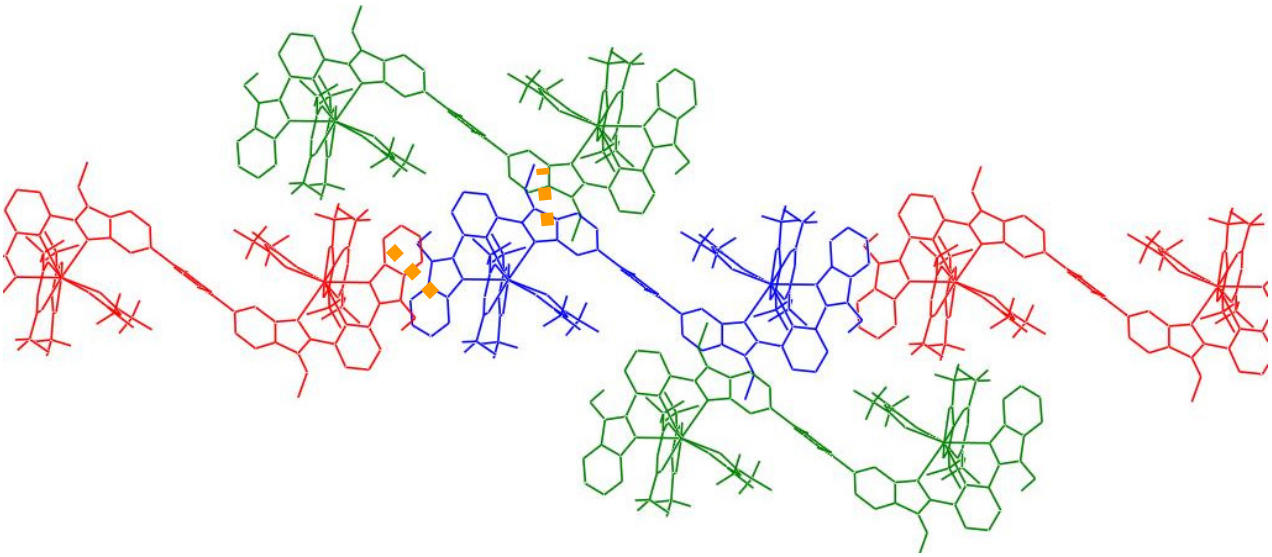

Figure S8 Intermolecular π-stacking interactions found in $[Eu_2(\mathbf{L4})(hfac)_6]$ (**4**) Each complex is involved in four intermolecular benzimidazole···benzimidazole interactions (d_1 = 3.49Å and d_2 = 3.87Å) with neighbouring molecules related by inversion centres.

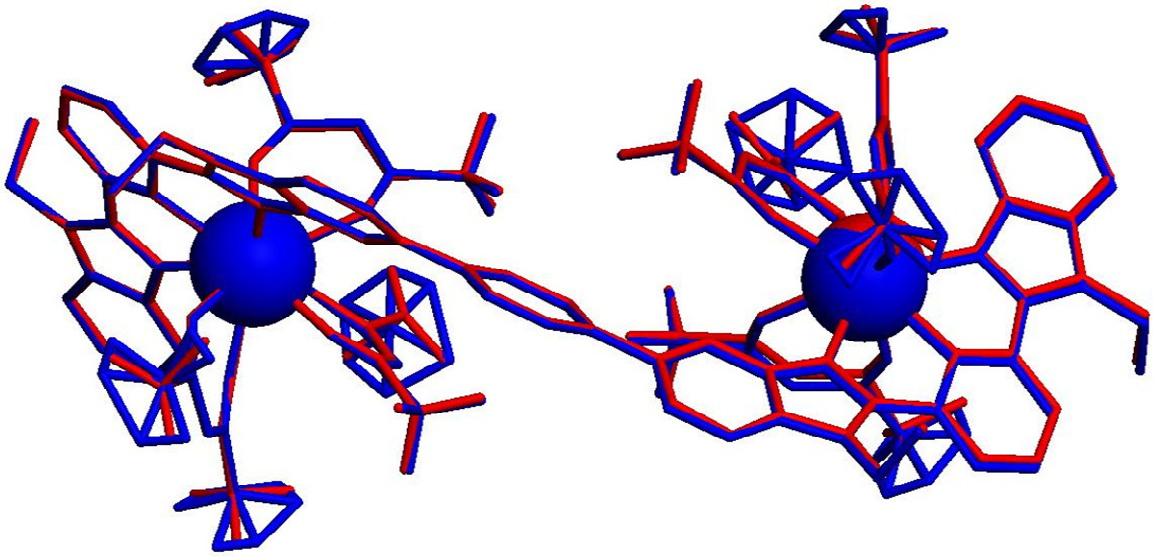

Figure S9 Superimposition of the molecular structures of $[Yb_2(\mathbf{L3})(hfac)_6]$ (red) and $[Y_2(\mathbf{L3})(hfac)_6]$ (blue).

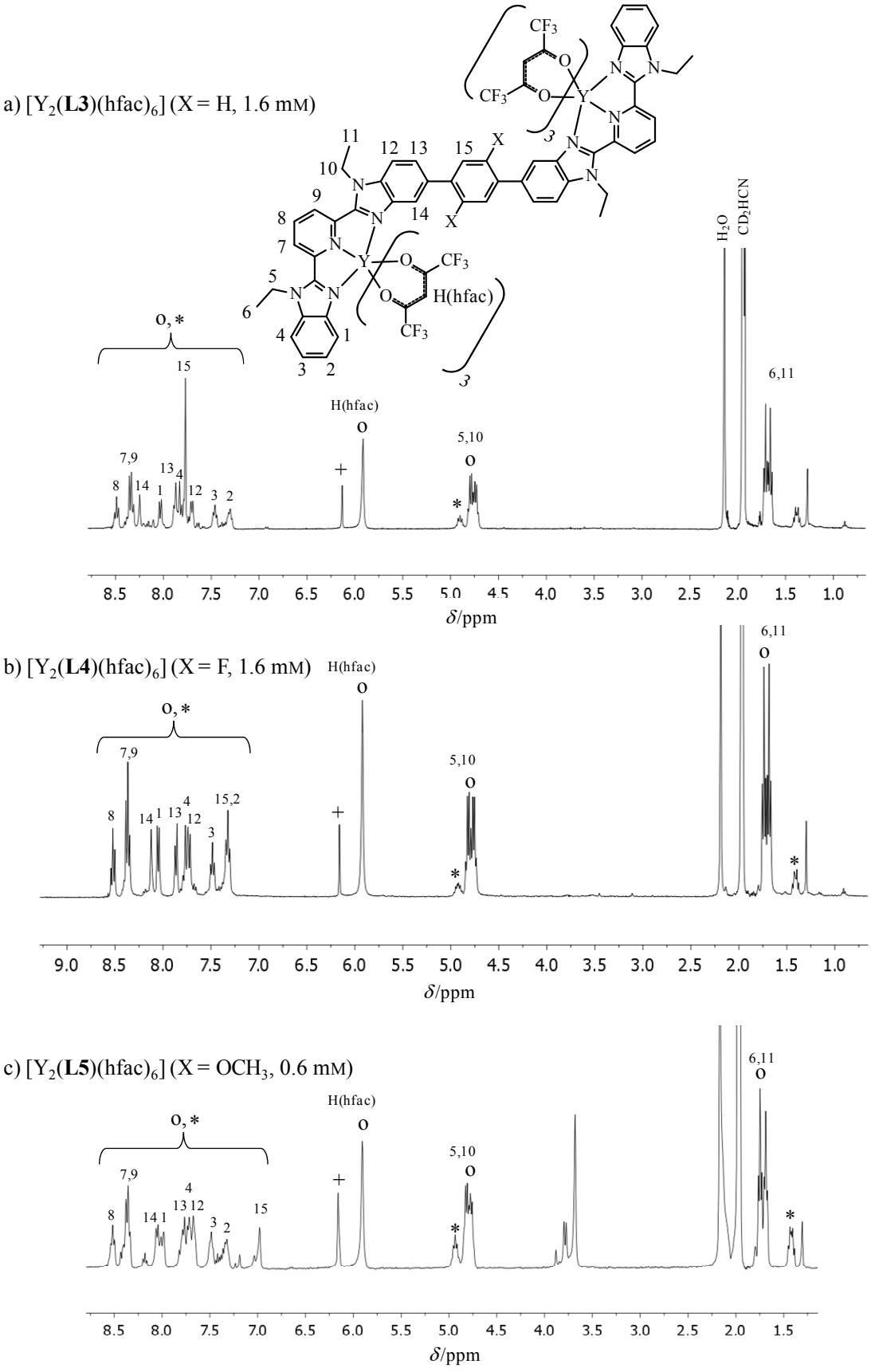

Figure S10 ^{1}H NMR spectra of the dinuclear complexes $[Y_2(\mathbf{L}\boldsymbol{k})(hfac)_6]$ (k = 3-5, CD_3CN, 293 K) with numbering scheme (o = $[Y_2(\mathbf{L}\boldsymbol{k})(hfac)_6]$, * = $\mathbf{L}\boldsymbol{k}$, + = $[Y(hfac)_3]$).

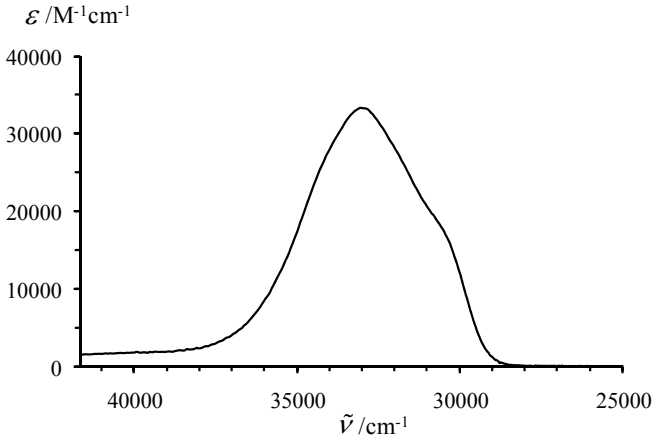

Figure S11 Electronic absorption spectrum of [Gd(hfac)$_3$(diglyme)] (10^{-4} M, CH_3CN, 293 K).

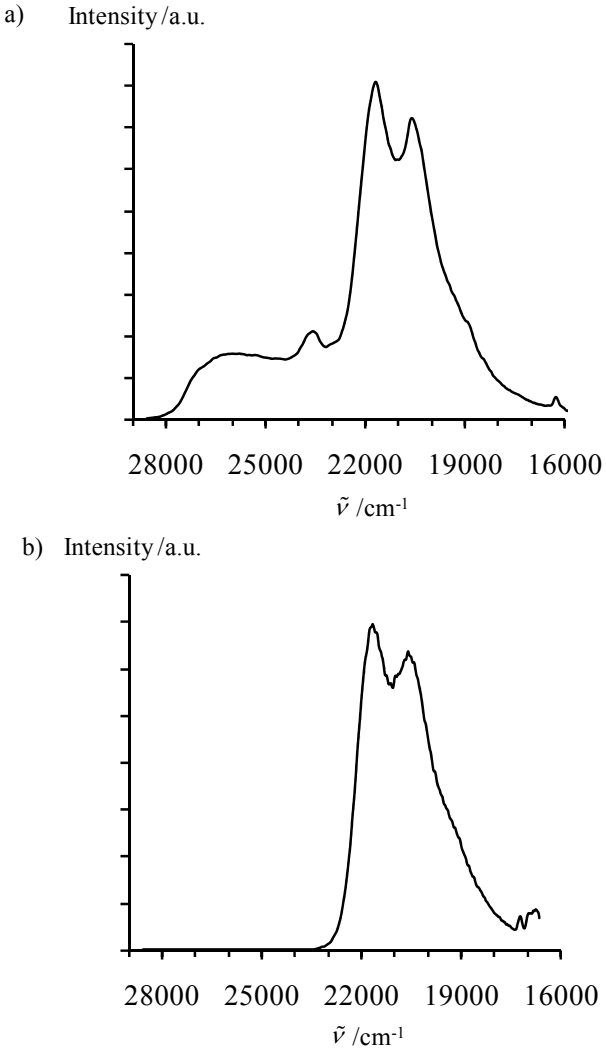

Figure S12 a) Fluorescence and b) phosphorescence (delay time 0.1 ms) emission spectra of [Gd(hfac)$_3$(diglyme)$_2$] (solid state, 77 K, $\bar{\nu}_{exc}$ = 32790 cm^{-1}).

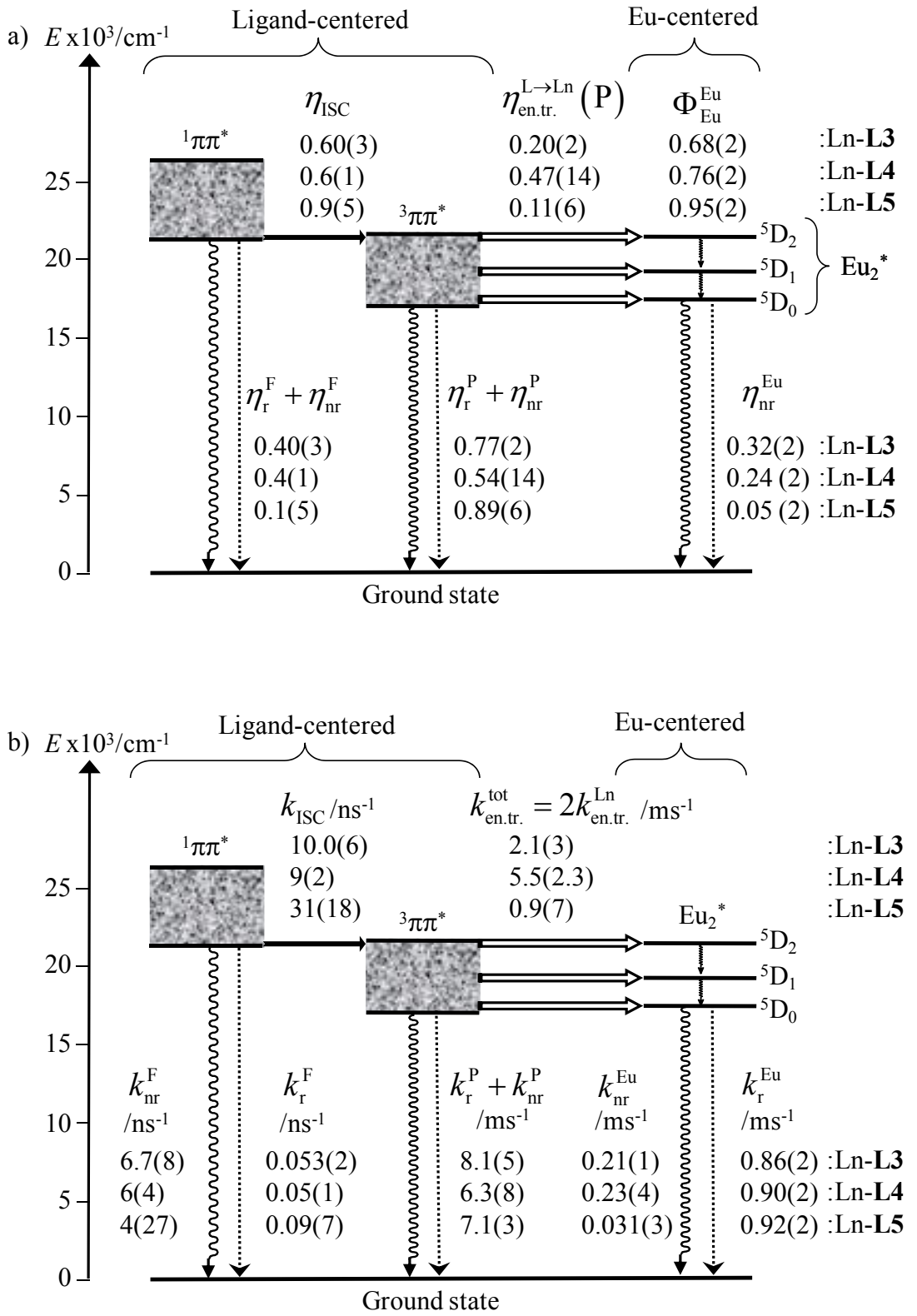

Figure S13 The figure shows the Jablonski diagram established for $[Eu_2(\mathbf{L}\boldsymbol{k})(hfac)_6]$ (k = 3-5) and collects a) the efficiencies and b) the rate constants for the global ligand-mediated sensitization of Eu(III) (solid-state, 293 K, method 1 in Table 4).

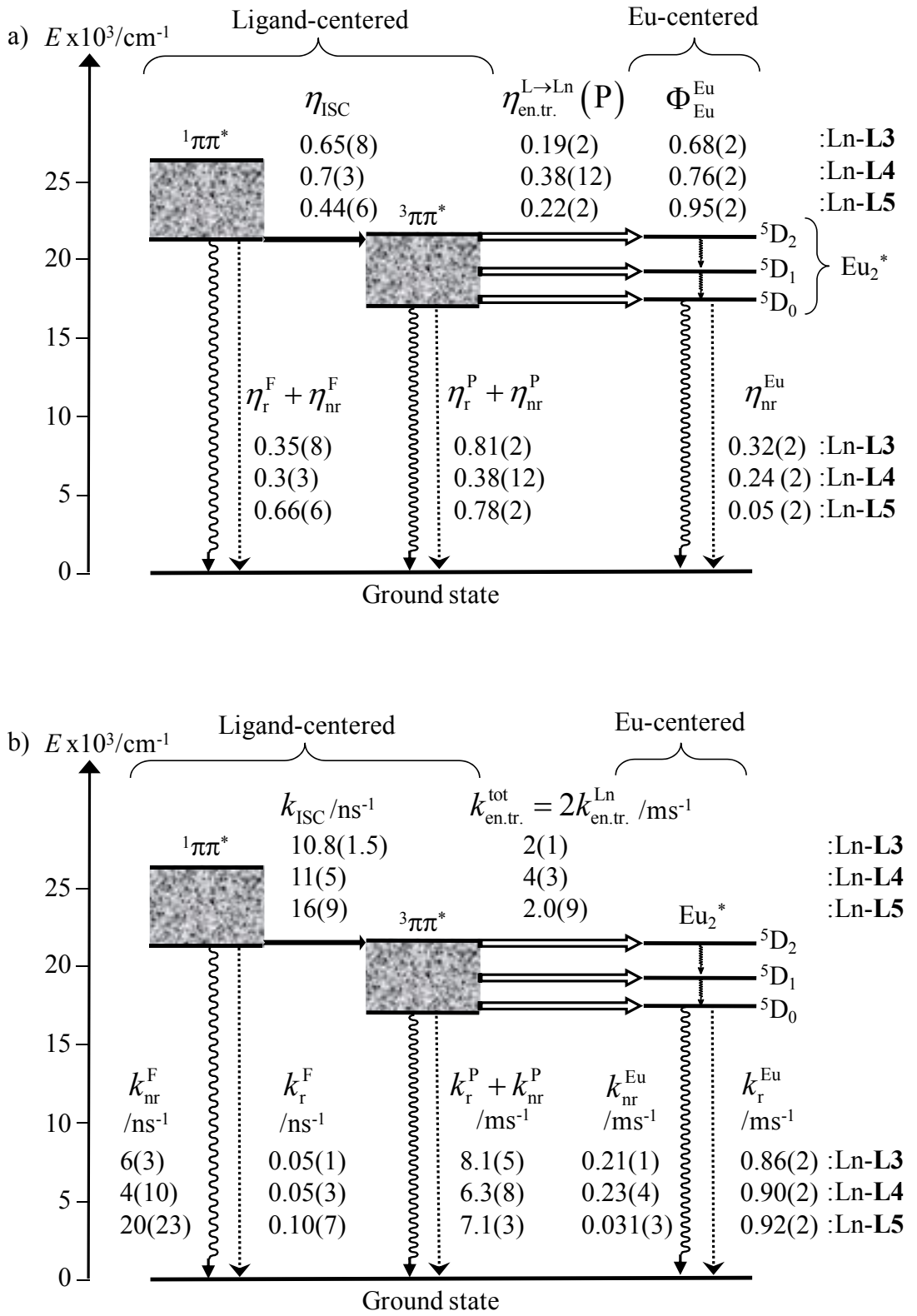

Figure S14 Simplified Jablonski diagram established for $[Eu_2(\mathbf{L}k)(hfac)_6]$ (k = 3-5) and collecting a) the efficiencies and b) the rate constants for the global ligand-mediated sensitization processes deduced from the measurement of the residual ligand-centred phosphorescence in the Eu(III) complexes (eqs 15 and 16, solid-state, 293 K, method 2 in Table 4).

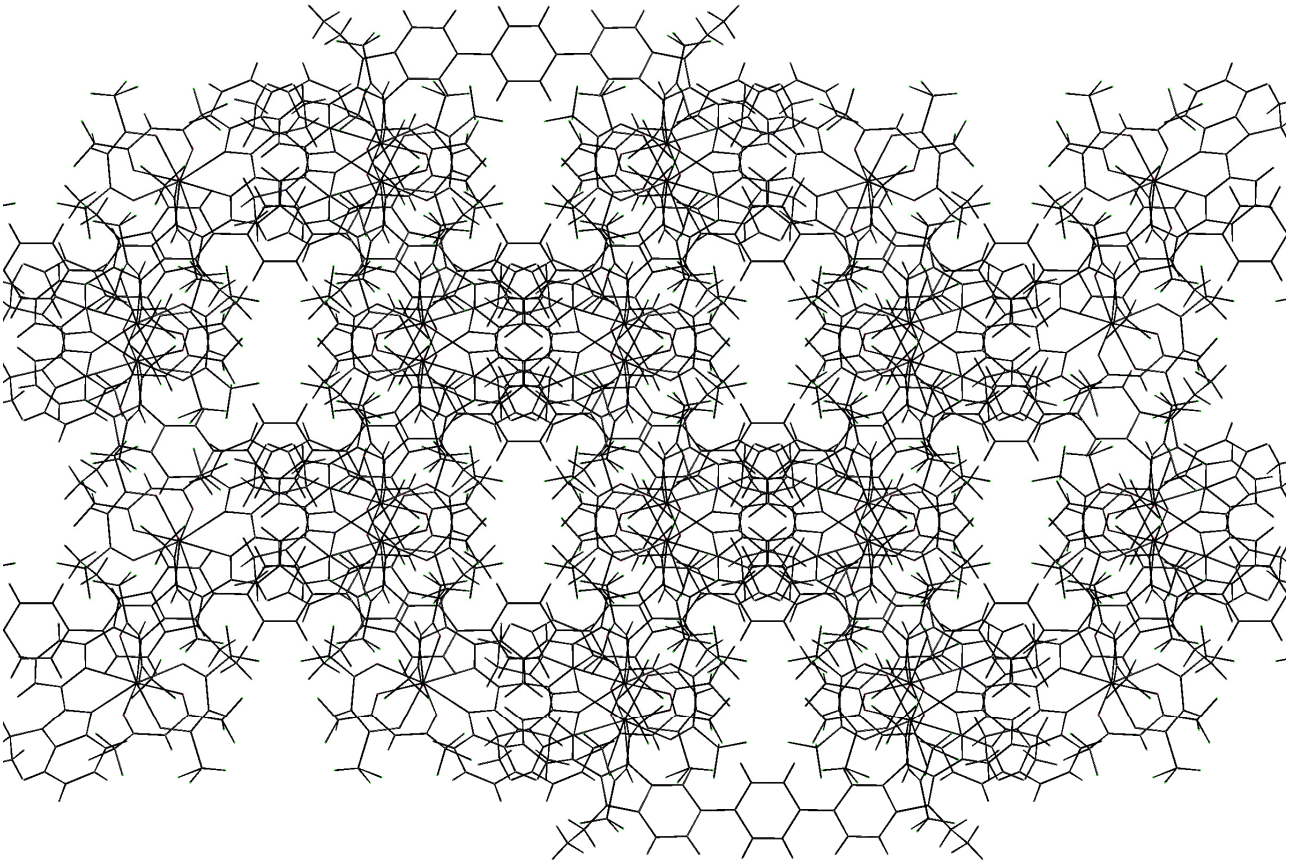

Figure S15 Crystal packing in the crystal structures of $[Ln_2(\mathbf{L3})(hfac)_6]$ (Ln = Yb, **1** ; Ln = Y, **2**) showing accessible voids (channels) along the [1 0 1] direction, where solvent molecules were highly disordered. Squeezed calculations were performed and the solvent-free structures were refined.